Available online at www.sciencedirect.com
ScienceDirect
Journal of Hazardous Materials 152 (2008) 757–764
Journal of Hazardous Materials
www.elsevier.com/locate/jhazmat

Application of chitosan as flocculant for coprecipitation of Mn(II) and suspended solids from dual-alkali FGD regenerating process

Zhong-Biao Wu, Wei-Min Ni, Bao-Hong Guan *

Department of Environmental Engineering, Zhejiang University, Hangzhou 310027, China

Received 11 March 2007; received in revised form 3 June 2007; accepted 16 July 2007
Available online 20 July 2007

Abstract

Heavy metals and suspended solid (SS) needed to be removed from the recirculation of dual-alkali flue gas desulfurization (FGD) system. The feasibility of coprecipitation of heavy metal and SS by water-soluble chitosan was studied in a lab scale experiment. The association between chitosan and metal ions was verified through DSC and FT-IR. The pH investigation revealed that at the pH ranged from 5 to 9, there were three stages for different actions: adsorption of chitosan for Mn(II), precipitation of manganese hydroxide and coprecipitation of manganese hydroxide and chitosan–Mn(II) complex. The ion selectivity experiments showed that the occurrence of Ca(II) in the solution had little influence on the adsorption of chitosan for Mn(II). The decrease rate of adsorption capacity was about 0.0023 mmol g^{-1} per 1 mg L^{-1} Ca(II). When adsorption and flocculation of chitosan occurred at the same time and at the sufficient addition of chitosan, chitosan not only made solids flocculate but also enhanced sorption capacity of chitosan. Application of chitosan for coprecipitation of Mn(II) and SS could remove Mn(II) efficiently and improve the settling characteristics of SS from dual-alkali FGD regenerating process.

Keywords: Chitosan; Flocculation; Manganese; Dual-alkali FGD

1. Introduction

Dual-alkali flue gas desulphurization (FGD) process was widely used in industry to reduce the effects of scaling and plugging of the lime/limestone-gypsum FGD process [1,2]. The process commonly employed initially a sodium carbonate solution to scrub SO_2 from the flue gas and then a lime slurry to regenerate the spent scrubbing solution to form $CaSO_3$ solids in the alkali solution (the slurry) [3]. So the regenerated slurry was formed in the regenerating process. The solids of the regenerated slurry were removed by sedimentation to produce a clear solution that was recycled for the scrubbing function at the pH ranged from 5.0 to 9.0. The clear solution could be re-circulated through the scrubber to remove SO_2 as an absorption solution and then could be regenerated again by the lime slurry.

The characteristic of the regenerated slurry was abundant in heavy metals (such as Mn(II), Zn(II), Ni(II), Cd(II)) besides high concentrations of suspended solid (SS). Heavy metals which came from coal-fired fume were dissolved into the absorbing solution and accumulated during the recirculation. At the present of dissolved heavy metals and oxygen sulfite in solution was oxidized [4]. The catalytic oxidation will make the absorbing solution ineffective and results in the decrease of desulphurization efficiency. So it was necessary for dual-alkali FGD process to separate SS and remove heavy metal ion from the regenerated slurry.

However, it was difficult to remove heavy metal ion from the slurry by conventional methods (such as chemical precipitation, ion exchange, adsorption, electrodeposition and membrane systems).

In recent years chitosan has been commonly used as chelate sorbents in heavy metals treatment from water and waste water and as flocculants in solid–liquid separation [5,6]. It was clear that chitosan was a good agent for chelating numerous trace metals from wastewater [7,8]. In most of cases, chitosan was mostly used to chelate metal ions in a variety of solid forms, such as beads, flakes and membranes [7–10]. The reason was that the interaction of metal ions with chitosan dissolved in the solution did not lead to the formation of settleable flocs and metal ions

* Corresponding author. Tel.: +86 571 87953088.
E-mail addresses: zbwu@zju.edu.cn (Z.-B. Wu), weimin_ni@163.com (W.-M. Ni), guanbaohong@zju.edu.cn (B.-H. Guan).

0304-3894/$ – see front matter © 2007 Elsevier B.V. All rights reserved.
doi:10.1016/j.jhazmat.2007.07.042

Nomenclature

B	weighted average settling velocity of flocculation based on their mass fractions ($m\,s^{-1}$)
C_{ab}	adsorption equilibrium concentration ($mmol\,L^{-1}$)
C_{eb}	background concentration of adsorption equilibrium ($mmol\,L^{-1}$)
F	mass fraction with a settling velocity less than or equal to U_s
Δh_i	descending height of water level (m)
H	height of settling column (m)
K	distribution ratio of Mn(II) adsorbed by chitosan to total removal Mn(II)
m	mass of dried solids (g)
M	mass of chitosan (mg)
$q_{(pH)}$	amount of Mn(II) adsorbed per chitosan ($mmol\,g^{-1}$)
U_{s,t_i}	settling velocity ($m\,s^{-1}$)
V	volume of liquid (mL)

remained bound onto the polymer but soluble in the solution [11]. It was necessary to get rid of the metal complex by a suitable filtration. The possibility of using water-soluble chitosans in decontamination of liquid radioactive wastes (LRW) of various origins from Co, Mn and Sr has been studied [12]. The result showed that chitosan in solution not only made solids flocculating but also enhanced sorption capacity of chitosan. So it was possible for water-soluble chitosan to remove metal ions. On the other hand chitosan had to be dissolved in the solution as flocculants. However, few reports in the literatures could be found on any application of the chitosan solution for simultaneous metal ion removal and suspended solid removal.

In this study, we attempted to consider the possibility of using a flocculation procedure with water-soluble chitosans for coprecipitation of heavy metal ions and SS from dual-alkali FGD regenerated process. After flocculating, SS could be separated easily and the concentration of metal ion could be lowered.

Since manganese ion was the secondary rich metal ion besides iron ion (shown in Table 1) and could predominate in the catalyzed oxidation of sulfite [13,14], it focused on the adsorption equilibrium of chitosan solution for Mn(II) ion. The influence of Ca(II) on the adsorption equilibrium was also studied because the concentration of Ca(II) was highest in the slurry.

Table 1
Metal ions in the regenerated slurry of dual-alkali FGD

Metal	Concentration ($mg\,L^{-1}$)	Metal	Concentration ($mg\,L^{-1}$)
Fe(II)	500–6000	Cr^{6+}	<0.1
Mn(II)	25–200	Cu^{2+}	<0.1
Sn(II)	0–10	Pb^{2+}	<0.1
Zn(II)	1–10	Ni^{2+}	0.1–5.0
Cd(II)	0.1–2.0		
Ca(II)	1000–3000	Mg^{2+}	500

Otherwise the effect of SS on the chitosan adsorption and the improvement of settling characteristics of SS by chitosan were considered. An approach to remove metal ions along with flocculating SS by chitosan was proposed.

2. Experimental method

2.1. Materials

Chitosan was purchased from Yuhuan Tianbao Chiotsan Co. Ltd., China. It was the product of deaceto-group chitin, with 85% *N*-acetylation degree and average molecular weight 1.0×10^5. The average molecular weight was determined in term of Mark–Houowink equation by intrinsic viscosity. Chitosan powder was accurately weighed 5.0 g and mixed with 500 mL of 1% acetic acids solution and kept agitating to accelerate the dissolution for about 2 h.

2.2. Procedure

2.2.1. Adsorption of chitosan for Mn(II)

The single heavy metal solutions were prepared for this experiment and contained 1 $mmol\,L^{-1}$ $MnSO_4$ with a range of 0–50 $mmol\,L^{-1}$ $CaCl_2$. The influence of pH and Ca(II) on the adsorption equilibrium was studied:

(1) *Adsorption of chitosan for Mn(II)*. The experiments were carried out in the batch mode for the measurement of adsorption capacities. The bottle with 250 mL capacity was filled with the single heavy metal solution and the chitosan solution. The mixed liquor was immediately adjusted to a certain pH value with 1% Na_2CO_3 solution or 0.5% NaOH solution. Some suspended solids happened to occur in the solution at pH >5.0. The bottles were shaken for more than 4 h at room temperature in a reciprocating shaker. The solid-liquid separation was carried out by filter papers. The solution was analyzed by atomic absorption spectrophotometer (AA-6300, Shimadzu, Japan), equipped with a flame atomizer (air/C_2H_2) and hollow cathode lamps of Mn. The Mn(II) concentration was determined at wavelength 280.0 nm. The adsorption equilibrium concentration was defined as C_{ab} in $mmol\,L^{-1}$.
(2) *Solubility of manganese hydroxide*. Due to metal hydroxide precipitation at high pH, other experiments were carried out without chitosan. The equilibrium concentration was the background concentration of adsorption equilibrium and was defined as $C_{eb(pH)}$ in $mmol\,L^{-1}$.
(3) *Characterization*. DSC and TGA were performed by using a DSC meter (Netzsch STA 409 PC, Germany). Approximately 20 mg of chitosan or chitosan–manganese complex was encapsulated non-hermetically in an alumina pan and scanned from 30 to 1000 °C at a heating rate of 10 °C per minute in dynamic N_2 atmosphere. All runs for the various samples were performed in duplication.

Fourier transform infrared (FT-IR) spectrometry (Nicolet Nexus 670) with an effective frequency range of 400–4000 cm^{-1}

was used to analyze chitosan and chitosan–manganese complex in KBr.

2.2.2. Coprecipitation of Mn(II) and SS with chitosan

The composite regenerated slurry was prepared by 10 g L^{-1} calcium sulfite solids with a range of 50 mmol L^{-1} $CaCl_2$ and 1 mmol L^{-1} $MnSO_4$. The influence of SS on the adsorption equilibrium and the settling improvement of the slurry with chitosan were studied:

(1) *Coprecipitation of Mn(II) and SS*. The well-stirred composite slurry 250 mL was transferred to a 500 mL beaker. Then the chitosan solution was added through a pipette. The mixed liquor was immediately adjusted to a certain pH value with NaOH solutions. After flocculating, the flocculation was transferred into the reservoir for the settling test. The solution was analyzed by atomic absorption spectrophotometer.
(2) *Settling tests*. Settling tests were performed in a top loading facility (Fig. 1), containing a settling column with 10 cm in diameter and 100 cm in height, an upper reservoir at the top to transfer the flocculation into the settling column and a sample cone at the bottom to withdraw the flocculation. The volume of the reservoir is about 250 mL. A flat was placed at the bottom of the reservoir and could be split with the reservoir.

First, water, at the room temperature, was added to the apparatus until its surface was as high as the top of the settling column. At start time the flat was split from the reservoir and the flocculation was allowed to fall into the settling column. Samples

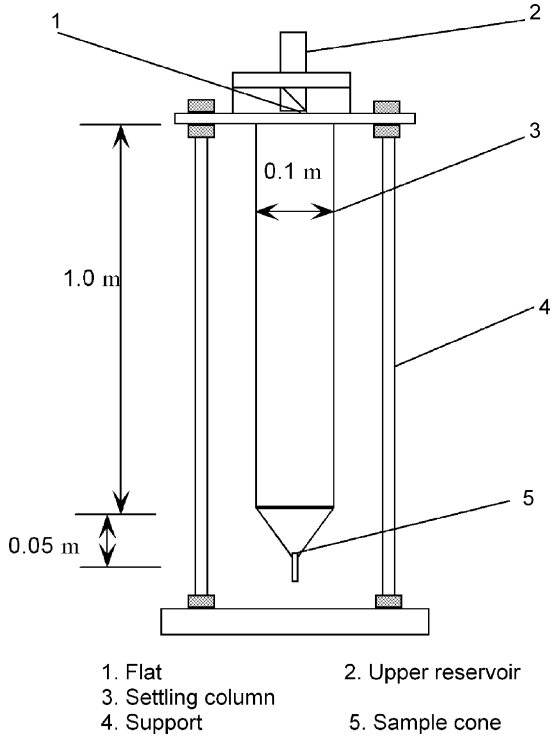

Fig. 1. A schematic of the top loading facility.

with the same volume of the cone were withdrawn from the tip of the cone at times $t_1, t_2, t_3, t_4 \ldots t_{i-1}$ and t_i. So the flocculation settling under the bottom of the cone between t_{i-1} and t_i could be withdrawn as the sample i at time t_i. In this case the settling velocity could be calculated by

$$U_{s,t_i} = \frac{H - \sum_{j=0}^{i-1} \Delta h_j}{t_i}, \qquad n \geq i \geq 1, \quad \Delta h_0 = 0 \tag{1}$$

where U_{s,t_i} is the settling velocity at time t_i, H the height of settling column, and Δh_i is the descending height of water level due to withdraw of the sample i at time t_i.

After filtering and drying in an oven at 105 °C for 2 h, each sample was weighted on an analytical balance. m_j is the mass of the sample j at time t_j.

3. Results and discussion

3.1. Adsorption of chitosan for manganese

3.1.1. Verification of chitosan–manganese complex by DSC and FT-IR

DSC was an effective tool in characterizing chitosan and its metal complex. TGA curves and DSC scans of chitosan and chitosan–manganese complex were shown in Fig. 2. Chitosan degrades in two stages. The first stage starts at about 40 °C with a weight loss of 10%. The second stage starts at 272 °C with a weight loss of 40%.

The chitosan–manganese complex showed two degradation stages like the pure chitosan. The first stage of both started at about 42 °C with a weight loss of 9% due to the loss of water. However the second degradation stage of chitosan–manganese complex took place at lower temperatures than that of the chitosan. This indicated that the chitosan–manganese complex was formed during adsorption and was less stable than the chitosan itself.

An endothermic peak centered on 76 °C can be assigned to the evaporation of adsorbed water and water ligands. Chitosan did not show any endothermic transition between room temperature and 200 °C, indicating the lack of any crystalline or other phase change during the heating process. The strong exothermic peak

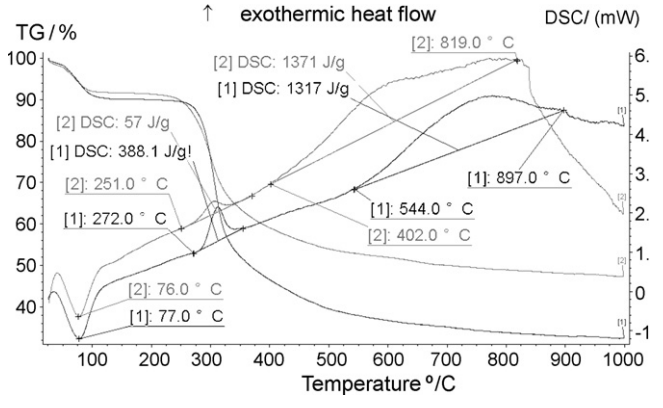

Fig. 2. TGA and DSC of pure chitosan (1) and chitosan–manganese complex at pH 7.0 (2) at a heating rate of 10 °C per minute in dynamic N_2 atmosphere.

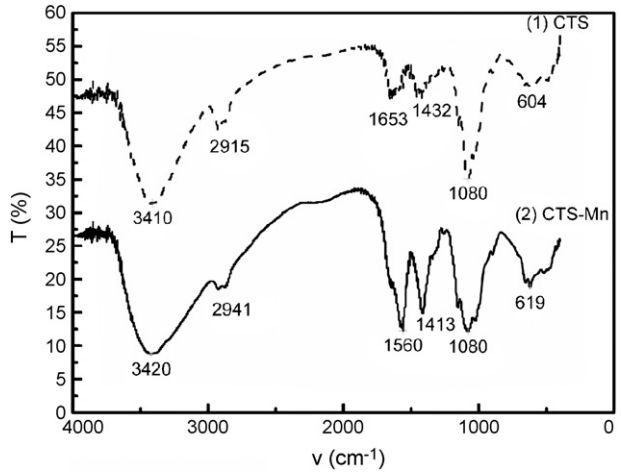

Fig. 3. FT-IR spectra of pure chitosan (1) and chitosan–manganese complex (2) with an effective frequency range of 400–4000 cm^{-1}.

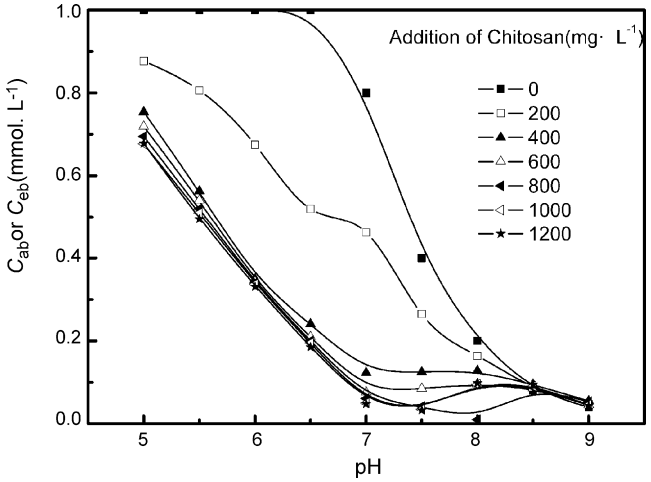

Fig. 4. pH effect on equilibrium concentration (C_{eb} or C_{ab}) of Mn(II) and chitosan–Mn(II) complex at different chitosan additions.

centered on 310 °C was due to the degradation of the chitosan [15]. However, the exothermic peak in the chitosan–manganese complex shifted to lower temperature.

Fig. 3 showed the FT-IR spectra of chitosan and chitosan–manganese complex. The spectra exhibited many alterations after Mn(II) ion adsorption. The major differences were: (1) in the spectra of chitosan, the wide peak at 3410 cm^{-1}, corresponding to the stretching vibration of $–NH_2$ group and –OH group, shifted to higher wave number (3420 cm^{-1}) significantly after Mn(II) ion adsorption. (2) The absorb band at 1653 cm^{-1} attributed to N–H group bending shifted to lower wave number (1560 cm^{-1}) significantly after Mn(II) ion adsorption. (3) The band of –OH group stretching at 1080 cm^{-1} had no change after Mn(II) ion adsorption. The results suggested that the NH group of chitosan was involved in a chelation process that affected the structural integrity of the polymer.

So, fronted exothermic peak in the chitosan–manganese complex could be a manifestation of these structural alterations. It was consistent with the Hao's report [16].

The analysis result of DSC and FT-IR verified that there was an association between chitosan and metal ions, which made chitosan chain of complex broken easier than that of chitosan itself.

3.1.2. pH dependency

Under different pH, a part of removal Mn(II) ions were caused by the precipitation for $Mn(OH)_2$, which could lead to the misunderstanding and inaccurate interpretation of adsorption. So it was necessary for studies on adsorption of Mn(II) to measure the equilibrium concentrations of Mn(II) in the solution at different pH. The results of the equilibrium concentrations of Mn(II) at the pH ranged from 5 to 9 were summarized in Fig. 4. The influence of chitosan additions on the equilibrium concentrations of Mn(II) was also shown in Fig. 4.

As seen from Fig. 4, it was observed that the precipitation of $Mn(OH)_2$ occurred at pH >6.5 without chitosan. However, when chitosan was added, coprecipitation of chitosan–Mn(II) complex and $Mn(OH)_2$ occurred at pH ≥5.0 and the equilibrium concentration of Mn(II) was lower than that without chitosan between 5.0 and 8.5. At pH >8.5 the equilibrium concentration of Mn(II) with the addition of chitosan was consistent with that without chitosan. It was assumed that the coprecipitation with chitosan had no influence on the balance between Mn(II) ion and OH^- in the solution. The decrease of the equilibrium concentrations of Mn(II) was only caused by the precipitation of chitosan–Mn(II) complex. So the amount of adsorbed Mn(II), $q_{(pH)}$ in mmol g^{-1} was obtained by the difference between $C_{eb(pH)}$ and $C_{ab(pH)}$ and calculated from

$$q_{(pH)} = \frac{(C_{eb(pH)} - C_{ab(pH)})V}{M} \quad (2)$$

where M is the mass of chitosan (mg) and V is the volume of liquid (mL).

Fig. 5 showed the relationship between pH value of the equilibrated solution and adsorption capacities of chitosan for Mn(II). It was observed that the adsorption capacities of the Mn(II) ions increased with increasing the pH value of the solution until a maximum and then decreased with an increase in pH value. The

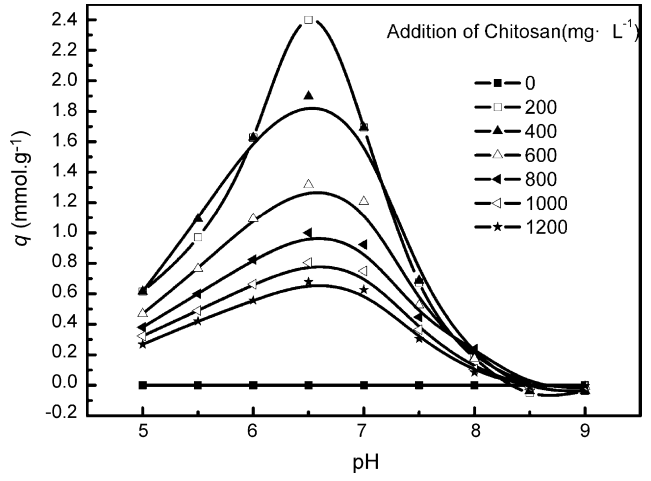

Fig. 5. Relationship between pH value and adsorption capacity (q) of chitosan for Mn(II) at different chitosan additions.

maximum adsorption of chitosan for Mn(II) in solution appeared at pH 6.5. These experimental results suggested that pH may be the dominant factor for adsorption of chitosan in aqueous media. It was also observed that the adsorption capacities of Mn(II) ions were very low at pH >8, due to the weaker electrostatic attraction by the protonated amino group of chitosan. The dissociation equation of the amine groups of chitosan had been described by Jha et al. [17]:

$$CM^{+} : H + H_2O \Leftrightarrow CM : + H_3O^{+} \quad (3)$$

where CM was represented as chitosan.

In acid medium, when the pH increased, the $–CH_2COO^{-}$ and $–NH_2$ groups were free from the protonation, and the adsorption capacities increased; the adsorption mechanism may be partially replaced by a chelation mechanism. It was apparent that chitosan was dissolved in acidic solution and was precipitated in alkalized solution. So alkalization could make chitosan provide the maximal adsorption capacity. However, in alkali medium, the formation of $Mn(OH)_2$ prevented further adsorption of chitosan for Mn(II) and the adsorption capacities decreased.

The distribution ratio, K was defined as the ratio of Mn(II) adsorbed by chitosan to total removal Mn(II) and was calculated by

$$K = \frac{C_{eb(pH)} - C_{ab(pH)}}{C_0 - C_{ab(pH)}} \quad (4)$$

where C_0 is the initial concentration of Mn(II) (mmol L^{-1}). The relationship between pH value of the equilibrated solution and K was shown in Fig. 6.

As shown in Fig. 6, there were three reaction stages during the pH range of 5 and 9. The first stage occurred before the formation of manganese hydroxide and K was close to 1. The adsorption of chitosan for Mn(II) could predominate in this stage. In the second stage, in which the pH ranged from 6.5 to 8.5 and K was between 0 and 1, the adsorption and coprecipitation of manganese hydroxide and chitosan–Mn(II) complex coexited. When pH >8.5, there was the third stage, in which K was close to 0. So the precipitation of manganese hydroxide could predominate and the adsorption could not occur. In order to make chitosan adsorb Mn(II) efficiently, the optimal pH was approximately 6.5.

3.1.3. Effect of dosage

The experimental results of six dosages revealed a definite increase in the adsorption capacity of chitosan with dosage. The larger number of available adsorption sites were favorable for the enhanced uptake of the metal ion. So the dependence of adsorption on dosages can be explained in terms of the concentration factor involving low ratio of metal ion to adsorbent at low metal concentrations. Subsequently, fractional adsorption became independent on initial concentration. However, at higher concentrations, the available sites of adsorption became fewer and hence the removal percentage of metal ion was dependent upon the initial concentration. From Figs. 4 and 6, on the basis of chitosan utilization ratio, the optimal dosage of chitosan was 600 mg L^{-1} and its adsorption capacity at pH 6.5 was 1.32 mmol g^{-1}. On the other hand, when pH >7.0, especially more than 8.5, the adsorption of chitosan decreased and the total removal efficiency of Mn(II) was determined by the solubility of $Mn(OH)_2$.

3.1.4. Ionic selectivity

In dual-alkali FGD regenerating process, the concentration of Ca(II) was highest in the slurry. These ionic selectivity tests were performed in the presence of $CaCl_2$ with different concentrations when pH was 6.5 and the dosage of chitosan was 600 mg L^{-1}. Fig. 7 revealed the effect of Ca(II) ion concentration on adsorption of chitosan for Mn(II).

Simultaneous adsorption resulted in a small reduction in Mn adsorption. The decrease rate of $q_{(pH)}$ was about 0.0023 mmol g^{-1} per mmol L^{-1} Ca(II). The reason was that alkaline and alkaline-earth metals had the absence of d and f unsaturated orbitals (unlike transition metals) [11] and chitosan was selective of transition metals over common non-transition metals. So Ca(II) could have holdback on the adsorption of Mn but had little influence on the adsorption.

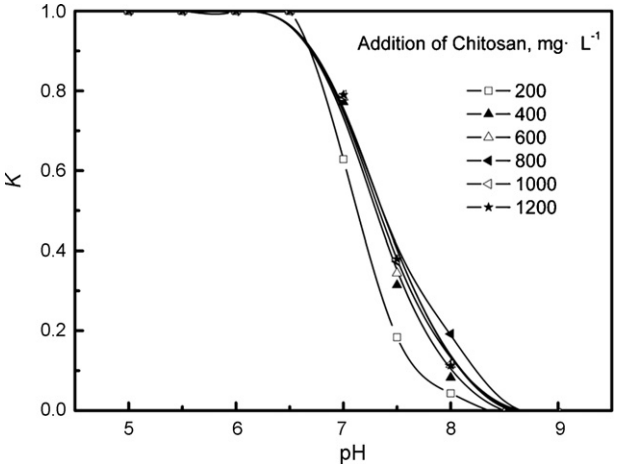

Fig. 6. Relationship between pH value and the distribution ratio (K) of Mn(II) at different chitosan additions.

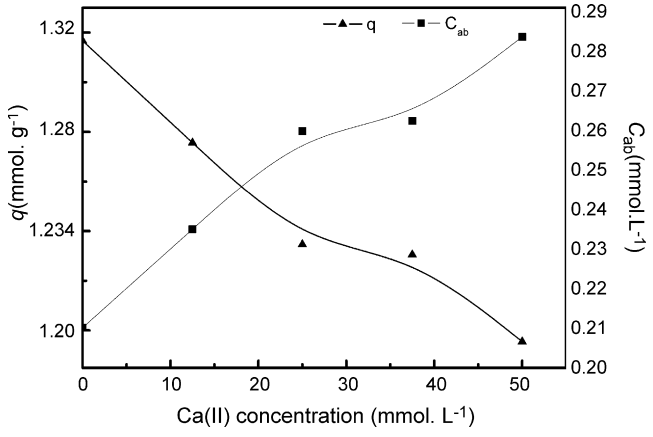

Fig. 7. Effect of Ca(II) ion concentration (pH 6.5, the dosage of chitosan was 600 mg L^{-1}) on equilibrium concentration (C_{ab}) and adsorption capacity (q) of chitosan for Mn(II).

Table 2
Data from the sedimentation of regenerated slurry were used in the development of the settling velocity curve

Sample number, i	Sampling time (min)	U_s (m s^{-1})	m_i (g)	F
1	0.5	0.0333	0.7336	1.000
2	2	0.00767	1.0271	0.940
3	4	0.00367	1.3349	0.856
4	7	0.00233	2.5998	0.746
5	10	0.00133	3.4610	0.533
6	15	8.47×10^{-4}	0.1827	0.249
7	25	5.93×10^{-4}	1.6947	0.234
8	30	4.43×10^{-4}	0.7998	0.095
9	60	2.58×10^{-4}	0.2773	0.029
10	120	1.20×10^{-4}	0.0791	0.006
11	240	6.60×10^{-5}	<0.0010	0.000

3.2. Coprecipitation of Mn(II) and SS with chitosan

Chitosan was used as not only chelate sorbents but also flocculants. When the regenerated slurry contained high concentrations SS, it could have effect on the adsorption of chitosan for Mn(II) ion. Otherwise, flocculation of chitosan for SS could improve its settling characteristic. The experiments were carried out at the optimum pH with different dosages of chitosan.

3.2.1. Flocculation of composite regenerated slurry

The results of the settling test for the composite regenerated slurry were summarized in Table 2. The distribution of settling velocity with mass fractions could be reflected in the plot with U_s and F as shown in Fig. 8. Here, F was the mass fraction with a settling velocity less than or equal to U_s and was given by

$$F(t_i) = 1 - \frac{\sum_{j=0}^{i-1} m_j}{\sum_{j=1}^{n} m_j}, \qquad n \geq i \geq 1, \quad m_0 = 0 \tag{5}$$

Flocculation tests were performed in the presence of different flocculant's dosages at pH 6.5. The results were shown in Fig. 9.

In order to describe solid's settling characteristic improvement by flocculation, it was necessary to have a mathematical description of the settling velocity curve. By using an iterative approach to find a least-square fit, it was observed that a nonlinear equation could fit well with the settling data obtained in settling tests. This equation was found to be suitable as follow [18]:

$$F = \frac{(A_1 - A_2)}{[1 + (U_s/U_0)^p]} + A_2 \tag{6}$$

The parameters of the settling velocities were summarized in Table 3.

So settling properties of the flocculated solids could be characterized as the weighted average settling velocity, B and could be calculated by

$$B = \int_0^1 U_s \, dF \tag{7}$$

where B was the area surrounded by the curve and the line $F = 1$, shown in Fig. 8.

By using Eqs. (6) and (7), B can be calculated and shown in Fig. 10. B increased with an increase of the dosage and tended to be a constant value. At low dosages, the floc size was very small due to the insufficient amount of flocculant's adsorption on solids. So the size distributions of the flocculation went near to those of the slurry without flocculating. When the dosage was less than 0.1 g L^{-1}, the settling properties of flocs were near to that of the slurry without flocculating. The increase in the

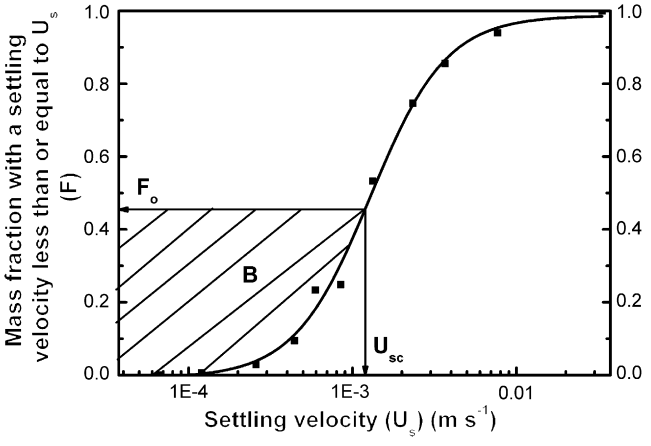

Fig. 8. Settling velocity curve of the composite regenerated slurry without flocculation (pH 6.5).

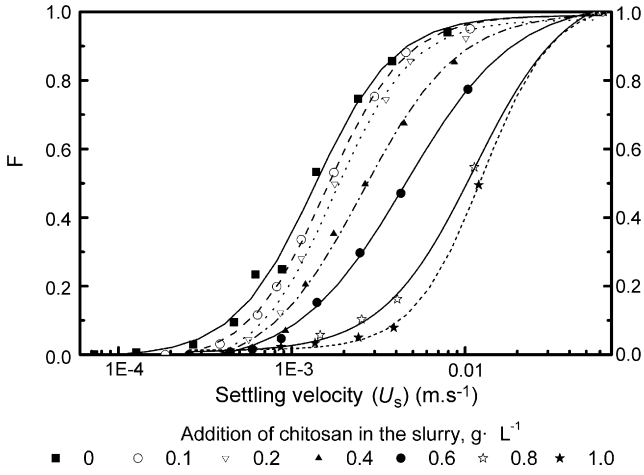

Fig. 9. Effect of the flocculant's dosage (pH 6.5) on settling characteristic (F, the mass fraction with a settling velocity less than or equal to U_s).

Table 3
Settling velocity curve parameters under different chitosan dosages for flocculated regenerated slurry

Chitosan dosage (g L^{-1})	Equation parameters				R^2
	A_1	A_2	U_0	p	
0	−0.0384	1.024	0.00134	1.876	0.995
0.1	−0.13182	1.024	0.00135	1.50538	0.988
0.2	−0.01189	1.004	0.002	1.91097	0.989
0.4	−0.02436	1.04099	0.003	1.51237	0.998
0.6	−0.02922	1.06321	0.005	1.32403	0.995
0.8	−0.02362	1.13768	0.01203	1.34351	0.996
1.0	−0.02362	1.09013	0.01334	1.57856	0.997

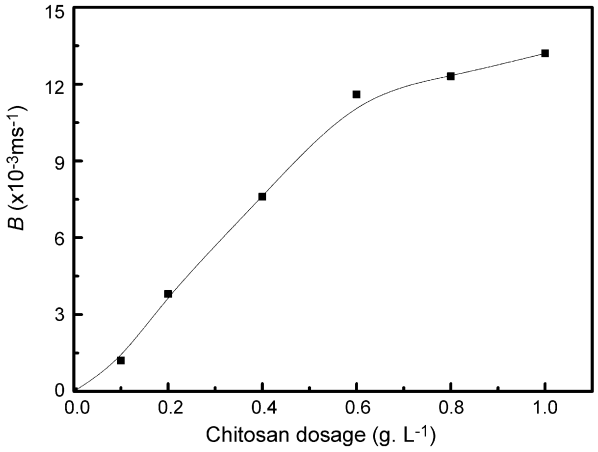

Fig. 10. Improvements of weighted average settling velocity (B) at different flocculant's dosage.

flocculant's amount would result in the incorporation of more suspended solids in a floc and in turn the enlarging floc led to the higher settling velocity. According to Fig. 10, the optimum value of B was $0.013\,m\,s^{-1}$ at a corresponding flocculant's dosage about $0.8\,g\,L^{-1}$. There were few differences between the optimum dosage of chitosan for adsorption and that of chitosan for flocculation.

3.2.2. Adsorption of chitosan with flocculation

When the SS in the composite slurry was flocculated by chitosan, Mn(II) ion in the slurry was also adsorbed by chitosan. The solution separated from the flocculated slurry was analyzed and Mn(II) concentration was determined. Fig. 11 sketched the comparison between the Mn(II) adsorption by chitosan with SS and without SS at pH 6.5.

From the results obtained above, it seemed that there was an insufficient addition of chitosan for adsorption on solids and Mn(II) ion at low dosages, especially less than $0.4\,g\,L^{-1}$. Due to the distribution of chitosan for flocculation, the adsorption capacity calculated was lower than that in single metal solution. It meant that chitosan has the higher ability to make solids flocculating than the ability to adsorb metal ion. With the increase of chitosan addition, the adsorption capacity in the composite slurry became more than that in single metal solution. The reason may be that the interaction of chitosan with solids may cause in the gelation of chitosan and the flocculation of the chitosan–Mn(II) complex [11]. In this case chitosan in solution not only made solids flocculating but also enhanced sorption capacity of chitosan.

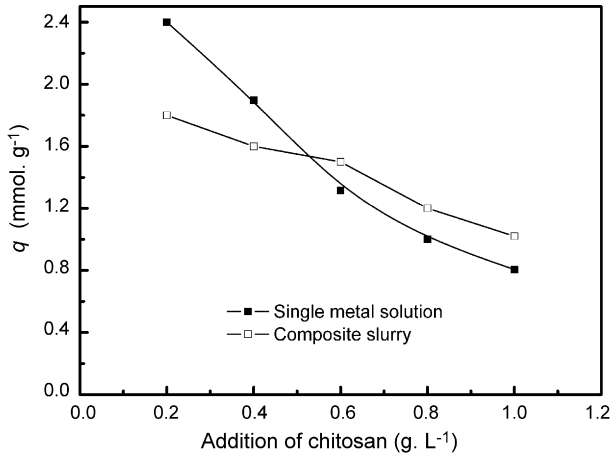

Fig. 11. Comparison between the adsorption capacity (q) of chitosan for Mn(II) with and without SS (pH 6.5).

4. Conclusions

From the above discussion, the conclusion can be reached that the application of chitosan for Mn(II) ion sorption simultaneous with flocculation in the dual-alkali FGD regenerating process was feasible. Chitosan could efficiently adsorb Mn(II) ion and remarkably improve the settling characteristic of SS. The primary conclusions resulting from this work can be summarized as follows:

(1) It was verified by DSC and FT-IR that NH group of chitosan was involved in a chelation process for metal ions. Experiments showed that chitosan in solution could adsorb Mn(II) ion and SS at the same time.
(2) There were three stages for different actions in the adsorption and coprecipitation of chitosan for Mn(II). The actions were depended on pH. The adsorption of chitosan for Mn(II) could predominate in low pH stage without formation of manganese hydroxide. In high pH stage, especially more than 8.5, manganese hydroxide precipitation occurred without adsorption. Between the two stages, there was the coprecipitation of manganese hydroxide and chitosan–Mn(II) complex.
(3) In the slurry, chitosan in the solution has the higher ability to make solids flocculating than the ability to adsorb metal ion. On the other hand, due to the interaction of chitosan with solids, chitosan in solution not only made solids flocculating but also enhanced sorption capacity of chitosan.
(4) The occurrence of Ca(II) in the solution had little influence on the adsorption of chitosan for Mn(II). The decrease rate of $q_{(pH)}$ was about $0.0023\,mmol\,g^{-1}$ per $mmol\,L^{-1}$ Ca(II) and was very small.

Acknowledgements

The research is financially supported by the National Hi-Tech Research and Development Program of China (863 Program, project no. 2001AA642030-1) and New Century Excellent Scholar Program of Ministry of Education of China (NCET-04-0549).

References

[1] J.C. Hower, U.M. Graham, A.S. Wong, et al., Influence of flue-gas desulfurization systems on coal combustion by-product quality at Kentucky power stations burning high-sulfur coal, Waste Manage. 17 (8) (1998) 523–533.
[2] J.S. Mo, Z.B. Wu, C.J. Cheng, et al., Experimental and theoretical studies on the desulfurization efficiency of dual-alkali FGD system in a RST scrubber, Chin. J. Proc. Eng. 6 (5) (2006) 54–59.

[3] C.R. LaMantia, R.R. Lunt, I.S. Shah, Dual alkali process for SO_2 control, AIChE Symp. Ser. 71 (148) (1973) 324–329.
[4] X.Q. Wu, Z.B. Wu, D.H. Wang, Catalytic oxidation of calcium sulfite in solution/aqueous slurry, J. Environ. Sci. 16 (6) (2004) 973–977.
[5] J.R. Deans, B.G. Dixon, Uptake of Pb^{2+} and Cu^{2+} by novel biopolymers, Water Res. 26 (4) (1992) 469–472.
[6] P.S. Strand, K.M. Vårum, K. Østgaard, Interactions between chitosans and bacterial suspensions: adsorption and flocculation, Coll. Surf. B 27 (1) (2003) 71–81.
[7] G. Mckay, H.S. Blair, A. Findon, Equilibrium studies for the sorption of metal ions onto chitosan, Ind. J. Chem. 28A (1989) 356–360.
[8] W. Kaminski, Z. Modrzejewsk, Application of chitosan membranes in separation of heavy metal ions, Sep. Sci. Technol. 32 (16) (1997) 2659–2668.
[9] G. Karthikeyan, K. Anbalagan, A.N. Muthulakshmi, Adsorption dynamics and equilibrium studies of Zn(II) onto chitosan, J. Chem. Sci. 116 (2) (2004) 119–127.
[10] J. Choong, H.P. Kwang, Adsorption and desorption characteristics of mercury(II) ions using aminated chitosan bead, Water Res. 39 (16) (2005) 3938–3944.
[11] E. Guibal, Interactions of metal ions with chitosan-based sorbents: a review, Sep. Purif. Technol. 38 (1) (2004) 43–74.
[12] V.N. Kosyakov1, I.E. Veleshko1, N.G. Yakovlev1, et al., Water-soluble chitosans as flocculants for deactivation of liquid radioactive wastes, Radiochemistry 45 (4) (2003) 403–407.
[13] W.L. Weisnicht, J. Overman, C.C. Wang, et al., Calcium sulfite oxidation in a slurry reactor, Chem. Eng. Sci. 35 (1980) 463–468.
[14] R. Yan, D. Gauthier, G. Flamant, et al., Thermodynamic study of the behavior of minor coal elements and their affinities to sulphur during coal combustion, Fuel 78 (1999) 1817–1829.
[15] J.C.Y. Ng, W.H. Cheung, G. McKay, Equilibrium studies of the sorption of Cu(II) ions onto chitosan, J. Coll. Interf. Sci. 255 (1) (2002) 64–74.
[16] H.Y. Hao, Q. Zhang, Q.K. Ge, Formation of Mn(II)with chitosan and molecular weight distribution of oligosaccharides by oxidating degradation, Chin. J. Inorg. Chem. 20 (9) (2004) 1085–1088.
[17] I. Jha, L. Iyengar, R.V. Prabhakara, Removal of cadmium using chitosan, J. Environ. Eng. 114 (4) (1988) 962–974.
[18] K.B. Wong, R.H. Piedrahita, Settling velocity characterization of aquacultural solids, Aquacult. Eng. 21 (2000) 233–246.